JOURNAL OF CATALYSIS 134, 615–628 (1992)

Metal-Support Interactions in Precipitated, Magnesium-Promoted Cobalt–Silica Catalysts

IMRE PUSKAS,* THEO H. FLEISCH,† JAN B. HALL,† BERNARD L. MEYERS,† AND ROBERT T. ROGINSKI†

Research and Development Department Amoco Chemical Company, †Amoco Corporation, Naperville, Illinois 60566

Received June 19, 1990; revised November 13, 1991

To define cobalt–silica interactions, precipitated, Mg-promoted catalysts were prepared by the cobalt nitrate–sodium carbonate reaction, without support and in the presence of silica supports. The major component of the unsupported Co catalyst was tentatively identified as Co_2CO_4 on the basis of elemental analyses and the IR carbonate absorptions at 1500 and ≈1400 cm^{-1}. Upon heating in air at 360°C, the unsupported catalyst converted to Co_3O_4 according to IR and XRD analyses. TPR studies indicated easy reduction at 300–400°C, with one peak for the Co_2CO_4 and the $Co(OH)_2$ components. A magnesium-promoted unsupported catalyst showed similar chemical properties and nearly identical IR spectrum; however, significantly different reducibility characteristics were observed by TPR. The composition of the silica-supported catalysts varied between two extremes. In the case of unreactive silica, IR and EM analyses showed a blend of the unsupported catalyst with the silica. In the other extreme, with reactive silicas, all the cobalt converted to cobalt silicates, as indicated by an Si–O stretching vibration at 1034 cm^{-1} and by the absence of carbonate absorptions. TPR traces of the blend-type catalysts were similar to their unsupported analogues. The cobalt silicates required temperatures >700°C for reduction according to TPR. The TPR of the intermediate-type catalysts that were, in part, blends of the unsupported catalyst with the silica and, in part, cobalt silicates showed cobalt silicate reductions starting above 400°C. This may be due to the catalytic effect of the cobalt that was reduced in the 300–400°C range. Electron microscopy, in combination with energy-dispersive X-ray analyses, further confirmed the cobalt–silica reaction. Cobalt silicates appeared as a "growth," often with a filamentous structure, leaving other areas of the silica completely intact. The formation of cobalt silicates by a solid–solute reaction is discussed.

INTRODUCTION

The "classical" hydrocarbon synthesis catalysts of Fischer and Tropsch were prepared by precipitation of cobalt and promoter compounds from the solutions of their nitrates using diatomaceous earth for catalyst support. These were used in commercial operations between 1935 and 1945. After the oil crises of the seventies, reports started to appear about active catalysts made by impregnation of porous silica (*1*). The differences between the catalysts made by different preparation techniques and on different supports are not well understood. Although numerous publications (*2–9*) appeared on the characterization of Fischer–Tropsch catalysts, only one of these (*5*) noted differences in the reducibilities of the Co/SiO_2 catalysts made by precipitation and by impregnation. Furthermore, we are unaware of studies that have addressed the cause of the reproducibility difficulties reported for the preparation of the precipitated catalysts (*2*).

We have studied the hydrocarbon synthesis process with cobalt-based catalysts, primarily with precipitated catalysts, and found that precipitated catalysts supported on high-surface-area silica were catalytically inactive. This was surprising because catalysts made the same way, but with dia-

0021-9517/92 $3.00

tomaceous earth supports (impure silicas with low surface areas), functioned reasonably well. This finding prompted us to study the role of the support. The supports, the unsupported catalysts, and the supported catalysts that were precipitated in the presence of the support were characterized by physical, chemical, surface chemical, and spectroscopic analyses to define changes attributable to interactions. We note that characterization of the unsupported catalyst was also required, because the published literature gives very little information on this subject except for stating that it is a basic cobalt carbonate. During the course of our work, the emphasis was placed on the definition of metal-support interactions, but we also attempted to identify other types of possible interactions (e.g., interactions with the promoters, surface carbons) that may influence the catalytic properties. This approach resulted in the unequivocal demonstration that silicas can react with the cobalt species under the slightly alkaline conditions of the precipitation, forming cobalt silicates. Particularly, reactive silicas (e.g., those having high surface areas) showed facile cobalt silicate formation.

EXPERIMENTAL SECTION

Materials. The cobalt nitrate hexahydrate and the magnesium nitrate hexahydrate were from J. T. Baker (both Baker Analyzed Reagents). The origins of the catalyst supports are given in Table 1. The $CoCO_3$ was from Alfa Products (technical grade); the Co_2SiO_4 from Pfalz & Bauer.

Catalyst preparations. The support (25 g) was slurried with stirring in a hot (80–85°C) solution of 30.9 g $Co(NO_3)_2 \cdot 6H_2O$ and 12 g $Mg(NO_3)_2 \cdot 6H_2O$ in 900 ml distilled water. A solution of 17.0 g Na_2CO_3 (anhydrous) in about 150 ml distilled water was added in 15 to 45 s. The pH of the solution changed from 5.4 to 8.4 during the precipitation. After a few minutes of additional stirring, the mixture was vacuum-filtered. The filter cake was reslurried in 900 ml of hot water by stirring and was filtered again. This washing step (reslurrying, filtration) was repeated twice. The final cake was vacuum-dried at 90°C and weighed. The cobalt was found to precipitate quantitatively. The cobalt contents of the catalysts (typically 17–18%) were calculated from the cobalt reagent weight and the catalyst weight. The weight fractions of the support were analogously determined and are shown in Table 3 (ignoring solubility losses and chemical reactions). The precipitation of the magnesium was found to be only partial. The magnesium contents of the catalysts were determined by inductively coupled plasma spectroscopy (ICP) and typically found to be in the 1.0–1.5% range. In the case of Catalyst 11 (see Table 3) the reagent quantities and ratios were changed to increase the cobalt and magnesium contents of the catalyst.

The various analyses (see below) were performed on catalyst samples prepared according to the above described procedures. Any additional catalyst treatment before analysis is reported in the description of the individual analytical technique.

Surface area and pore size distributions. Nitrogen physical sorption analyses were completed on a Digisorb 2600 and mercury porosimetry was performed on a 9220 Porosimeter (Micromeritics Corp.). The samples were outgassed under vacuum at 250°C. With lower outgassing temperature (50 or 100°C), the same or slightly lower surface areas were measured even with samples expected to undergo thermal decompositions at 250°C (i.e., with cobalt carbonate-containing samples). Conventional procedures were followed on data accumulation and reduction.

XRD. Analyses were performed on a Scintag PAD V diffractometer operating at 40 kV, 30 mA with a scanning speed of 0.3° per minute and 0.02° steps. Divergence slits of 0.2° and 0.4° were used with receiving slits of 0.5° and 0.3°. An energy-dispersive detector was employed on an unfiltered radiation.

TPR. Experiments were carried out in a home-built device based on the design by

Gruber (*10*). It consisted of a programmable furnace, a $\frac{1}{10}$-in. sample tube, appropriate valves for passing different gases over the samples, a dosing loop for pulse chemisorption, traps for the removal of H_2O and CO_2, and a thermal conductivity detector. Sample size (20 to 90 mg) was adjusted so that the cobalt content of the sample would remain approximately constant. The samples were dried and degassed under dry He stream at 100°C, cooled to ambient temperature, followed by programming at 5°C per minute in 20% H_2/80% N_2 to 380 or 800°C, after which there was an isothermal hold treatment. The hydrogen uptakes were calculated for the known cobalt contents assuming divalent state.

Electron microscopy (EM). Samples were studied on a Phillips 420T analytical electron microscope. This instrument was operated both in the transmission mode and the scanning transmission mode. The microscope was equipped with a Tracor Northern energy-dispersive X-ray analyzer (EDX), which can detect oxygen and heavier elements. The X-ray microanalyses were done in the scanning transmission mode with a fine diameter probe (100–200 Å). The samples were prepared for electron microscopy by embedding in epoxy and sectioning with an ultramicrotome.

IR and Raman spectroscopy. Transmission IR spectra were recorded on a Perkin–Elmer 1420 or a Mattson Nova Cygnus 120 FTIR instrument, either on Nujol and Fluorolube mulls (split technique), or on KBr pellet. The KBr pellets were dried *in vacuo* at 100°C before recording the spectra. The diffuse reflectance IR spectra (DRIR) were recorded on a Mattson Cygnus 100 FTIR spectrometer, utilizing an MCT A detector and a Harrick diffuse reflectance accessory. A total of 1024 scans at 8 cm^{-1} were coadded to obtain the final DRIR spectrum for each sample. The Raman spectra were obtained on an ISA Ramanor U1000 system. Data were obtained every 2 cm^{-1} at a 1 cm^{-1} slit resolution for the region 100–1500 cm^{-1}. A total of two scans were collected and coadded to obtain the final spectrum of each sample.

XPS. An HP ESCA 5950 spectrometer was used, having an attached reactor for *in situ* reductions. The catalysts were analyzed either as received, or after 2-h reductions at 380°C in flowing pure H_2. Monochromated Al$K\alpha$ radiation (hv = 1486.6 eV) was used as the excitation source and an electron beam with an energy below 10 eV was employed to minimize sample charging. The following photoelectron spectra were acquired: Co 2*p*, Si 2*p*, O 1*s*, C 1*s*, and Mg(KLL). The C 1*s* line at 284.6 eV was used for reference.

Elemental analyses. The carbon and hydrogen analyses were performed by Leco 600 analyzer by standard procedures. The carbonate carbons were determined on a UIC automatic CO_2 Coulometer (*11*).

RESULTS

Characterization of the supports. Table 1 summarizes the salient characteristics of the supports from nitrogen adsorption and infrared and X-ray photoelectron spectroscopic (XPS) studies. The supports include high-surface-area silicas 1–3 and, for comparison, commercial grades of diatomaceous earths 4 and 5 that were frequently used for catalyst preparation. These last two samples were 88–94% pure silicas. As shown in Table 1, the high-surface-area silicas had large mesopore volumes. The diatomaceous earths 4 and 5 had low surface areas and very little mesopore volume. However, mercury porosimetry indicated macroporosity for the diatomaceous earths (e.g., 2.2 cc/g for 4).

The supports were also characterized by IR spectroscopy. The strongest peaks assigned to Si–O stretching vibrations had broad maxima around 1100 cm^{-1}. A comparison of the spectra of the supports 1–5 revealed only minor differences. The silica gels 1–3 showed more intense –OH absorptions in the 3700–3100 cm^{-1} region, which is attributable, in part, to higher concentration of surface hydroxyls and, in part, to higher moisture content. A very small peak

TABLE 1

Characterizations of the Silicas Used as Supports

ID No.	Silica trade name, supplier	By N_2 adsorption		By IR	By XPS	
		Surf. A. (m^2/g)	Pore Vol. (cc/g)	Si–O (cm^{-1})	Atomic %	Surface carbon
					Total C	Carbonate C
1	Cab-O-Sil HS-5, Cabot	300	0.72	1113	11.7	3.5
2	CS 2133, P.Q. Corp.	320	2.04		2.3	
3	952 silica, Davison	279	1.56	1111	4.6	1.1
4	Filter-Cel, Manville	17	0.05	1100	8.1	0.2
5	Celite-219, AW,[a] Manv.	2.3	0.002	1100	9.3	<0.4

[a] AW, Acid washed, i.e., treated with 10% nitric acid at 95°C, followed by thorough washing with water and drying.

appeared in the FTIR spectra at 3748 cm^{-1} that is characteristic for isolated Si–OH. The high surface supports 1–3 exhibited a small extra peak at 973 cm^{-1}. A peak appearing in all spectra at 802 cm^{-1} was broader and slightly shifted in support 1.

Further characterizations were by XPS. The surface compositions were measured. In the high surface silicas 2 and 3, only trace C and Na surface impurities were found. In Filter-Cel 4, C, Al, Na, K, Ca, and Fe were detected. The carbon species were of particular interest because they can be potential precursors to cobalt carbides and to graphitic carbons. Formation of cobalt carbides (*12*) and deposition of graphitic carbon (*13, 14*) via the adsorption of CO on Co are well-established reactions; hence we were alerted to possible similar reactions with other sources of carbon. XPS can differentiate the carbon species on the basis of their binding energies as graphitic or carbidic or hydrocarbon type (284.6 eV), as oxygenated organic (286.6 eV) and as carbonate carbons (288.7 eV). Table 1 shows the total carbon content and the carbonate carbon content of the supports.

Characterization of the unsupported catalyst. An earlier investigation on the rapid precipitation of inorganic carbonates (*15*) has indicated that nonstoichiometric basic carbonates form most often, with loss of carbon dioxide. We have precipitated cobalt carbonates from cobalt nitrate solutions with sodium carbonate. Two of the precipitations were carried out in the presence of magnesium nitrate, to make "promoted" catalysts. The characterizations of the resulting materials are shown in Table 2. Nitrogen adsorption measurements indicated high surface areas and high pore volumes. Elemental analyses indicated approximately 2.5 : 1 and 2 : 1 atomic Co : C ratios for the cobalt and the magnesium-promoted cobalt catalysts, respectively. These catalysts were found to be essentially amorphous by XRD. The observed weak patterns were usually unsatisfactory for characterization. In the promoted catalyst 8, however, Co_3O_4 was identifiable as a trace component from its characteristic diffraction lines.

Heating the catalysts of Table 2 in air at 360°C for 2 h resulted in chemical conversions into mixed cobaltous–cobaltic oxide (Co_3O_4) that was identified by its characteristic XRD pattern and also by its IR spectrum. The weight loss that accompanied the thermal air oxidation of 7 was also measured by thermogravimetric analysis as 23.8%. The thermally oxidized samples were analyzed for their carbon and hydrogen content. After 1.5 at 360°C, 1.12% C and 0.65% H were found. After 3 h at 360°C, 0.88% C

TABLE 2

Characterizations of the Unsupported Catalysts

ID No.	Metals in catalysts	By N_2 adsorption		By elemental analyses			
		Surface A. (m^2/g)	Pore Vol. (cc/g)	Weight percent			
				Co	Mg	C	H
6	Co only			62	—		
7	Co only	132	0.78	57	—	4.56	1.70
8	Co plus Mg	271		47	3		
9	Co plus Mg	165	0.64	48		4.97	1.95

was found by carbonate carbon determination (*11*). These results indicate that residual carbon remained in the samples even after long exposures and that a quantitative conversion of the catalyst to Co_3O_4 was not achieved.

The unsupported catalysts were also analyzed by IR spectroscopy. The cobalt catalysts 6 and 7 and the magnesium-promoted catalysts 8 and 9 showed almost identical spectra (see Fig. 1). The most intense absorptions were at 1500 and at 1400–1386 cm^{-1}. These maxima are attributed to carbonates of some unusual structure, because they are outside the 1460–1400 cm^{-1} range reported for inorganic carbonates. A careful look at the shape of the carbonate peaks reveals two inflections at 1430 and 1460 cm^{-1}. By recording the IR spectrum of authentic $CoCO_3$, we have demonstrated that the two inflections coincide with the major peaks of $CoCO_3$. On this basis, $CoCO_3$ is a minor component of the unsupported cobalt catalyst.

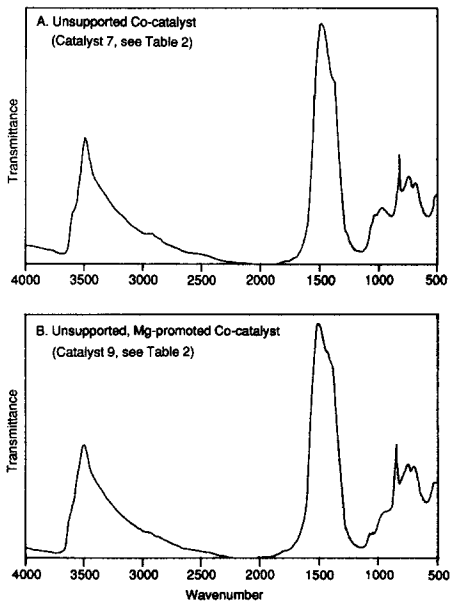

FIG. 1. FTIR spectra of the unsupported catalysts in KBr pellets.

These analytical results suggest that during the precipitation of the catalysts a mixture of compounds form, with an unknown cobalt carbonate species as the major component. The Co_2CO_4 structure is proposed for this species on the basis of elemental analyses and the observed carbonate IR frequency shifts. Either formula 15 or 16 (see Scheme 1) is possible. For the pure cobalt catalysts 6 and 7, the elemental analyses were poorly reproducible (see Table 2) and were found to be sensitive to the conditions of the precipitation and the drying temperature. The color of the various preparations also differed, from purple to nearly black. However, the IR spectra of 6 and 7 appeared identical. Since CoO is known to be IR-inactive (*16*), it is reasonable to assume that the CoO content varied in catalysts 6 and 7. The Raman spectra of 6 and 7 revealed a feature at 696 cm^{-1} that may be attributed

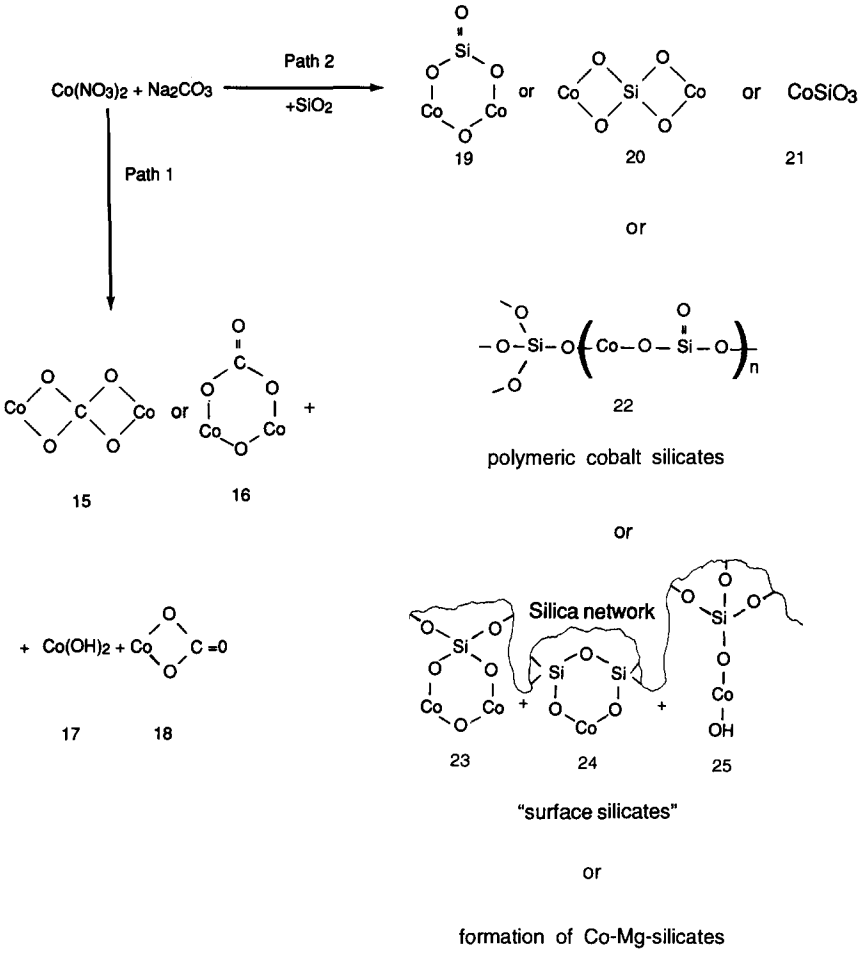

SCHEME 1. Possible reactions during catalyst preparation.

to CoO. However, this finding does not provide unequivocal evidence for CoO, because the Co_2CO_4 component of the mixture is also expected to absorb in this region.

The reducibilities of the unsupported catalysts were studied by TPR. The unsupported cobalt 7 easily reduced at low temperature (<420°C) and showed only one maximum in its TPR curve (see Fig. 2a). This finding suggests that the Co_2CO_4 and the CoO components reduce approximately at the same temperature and the same rate. This may not be surprising if we consider that the Co_2CO_4 may have decomposed first to CoO and CO_2, before the reduction occurred. Hydrogen consumption was 116% of the theoretical, indicative of a quantitative cobalt reduction. The Mg-promoted catalyst 9 showed a considerably different TPR curve (see Fig. 2b). Several maxima were observed and there was quite substantial hydrogen uptake at high temperatures. These results could be explained by assuming the formation of mixed salts between the Co and the Mg, which reduced at different temperatures and at different rates than the pure cobalt species. The measured total hydrogen uptake was 116% of the theoretical, suggesting again a quantitative reduction.

Characterizations of the supported cata-

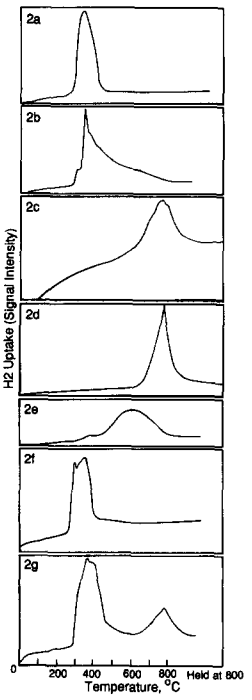

FIG. 2. Hydrogen consumptions by the various catalysts during temperature-programmed reductions.

lysts. Table 3 summarizes some of the properties of the supported catalysts. Catalysts 10–12 were made on high-surface-area supports. These possessed higher surface areas than their respective supports. Catalysts 13–14 were prepared with a low-surface-area support. These had much lower surface area than catalysts 10–12.

The reducibilities of the catalysts were studied and measured by XPS and/or TPR. Many of these studies were limited to 380°C reduction temperature to obtain information about reducibilities under industrially favored conditions. Table 3 gives the extent of cobalt reductions at 380 and 800°C. As the data of Table 3 show, XPS did not detect cobalt reductions at 380°C in catalysts 10–12. The TPR traces of Figs. 2c and 2d did not indicate low-temperature hydrogen uptakes either; temperatures above 700°C were required. A quantitative reduction of these catalysts was not even achieved at 800°C (see Table 3). As shown in Fig. 2e and Table 3, in catalyst 13, a small degree of reduction occurred below 400°C, but the bulk of the material required 500 to 750°C for reduction. Catalyst 14 reduced completely below 400°C (see Table 3 and Fig. 2f). The species reducible below 400°C can be assigned to carbonates and oxides of cobalt, while the species requiring temperature above 700°C are believed to be cobalt silicates (*9*). In order to learn the identity of the species reducing at 500–750°C in catalyst 13, the following working hypothesis was advanced: It was assumed that the same silicate species were present in catalyst 13 as in catalyst 10–12, but, in catalyst 13, reduction was facilitated by the presence of metallic cobalt generated from the reduction of the oxides–carbonates. To test this hypothesis, a 1 : 1 blend of catalysts 12 and 14

TABLE 3

Characterizations of the Supported Catalysts

ID No.	Support No.	Support content (wt%)	By N_2 adsorption		By % Co reduction		
			Surface A. (m^2/g)	Pore Vol. (cc/g)	By XPS (380°C)	By TPR (380°C)	By TPR (800°C)
10	1	71	342	0.44	0	—	56
11	2	60	452	0.27	0	—	—
12	3	72	427	0.71	0	—	75
13	4	70	74	0.10	0	5.3	105
14	5	70	53	0.17	—	103	113

was analyzed by TPR. As Fig. 2g reveals, the TPR traces differed substantially from that resulting from the superimposition of Figs. 2d and 2f. A substantial amount of hydrogen uptake can be observed between 400 and 700°C, in contrast to Figs. 2d and 2f. Furthermore, the intensity of the high-temperature peak was clearly reduced. These results suggest that our hypothesis may be correct, but further work would be required to provide unambiguous identification of the species that reduced in the 500–750°C region.

All the catalysts of Table 3 were found to be essentially amorphous by XRD analysis. Catalysts 13 and 14 showed the presence of very low concentrations of crystalline silica (cristobalite, quartz), which were shown to originate from the diatomaceous earth support 4 and 5. Catalysts 10–14 were exposed to air oxidations at 360°C in an attempt to convert the cobalt species to Co_3O_4. Catalysts 10–12 remained amorphous to X rays after the air oxidations. Because Co_3O_4 is known to form large crystallites readily detectable by XRD, it can be inferred that catalysts 10–12 did not oxidize to Co_3O_4. This conclusion was confirmed by IR analyses: the characteristic absorptions of Co_3O_4 at 573 and 668 cm^{-1} were not observable in the air-oxidized samples. Surprisingly, not even catalyst 13 showed the presence of Co_3O_4 after heating in air, except for trace levels. Only catalyst 14 converted to Co_3O_4 upon 360°C heat treatment in air, as confirmed by XRD and IR analyses.

Catalysts 10–14 were also characterized by their IR and/or DRIR spectra. Apart from some anticipated relative intensity changes, the IR and the DRIR spectra were essentially identical. Figure 3 shows the IR spectrum of catalyst 14. The broad absorption band at 1500–1380 cm^{-1} is the carbonate absorption that was found in the unsupported catalysts. The 1090 cm^{-1} maximum is assigned to the Si–O stretching vibration of the support. There was no sign of an absorption maximum around 1040 cm^{-1}, where some of the other catalysts had a new

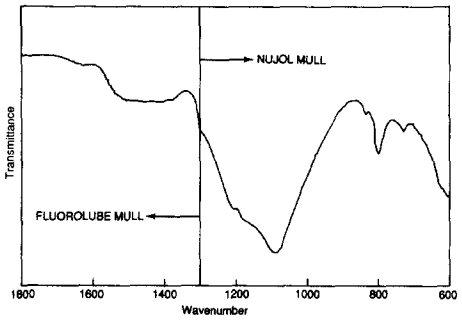

FIG. 3. Partial IR spectrum of catalyst 14 (split technique, in Fluorolube and Nujol Mulls).

maximum. Figures 4 and 5 compare the DRIR spectra of catalysts 12 and 13 to those of their respective supports 3 and 4. In Figure 4, the carbonate absorptions were not present. In the Si–O stretching region, a new maximum appeared in the spectrum of catalyst 12 at 1034 cm^{-1}. This absorption indicates chemical changes in the support. The maximum was shown to coincide with that of authentic Co_2SiO_4. These results clearly show the presence of cobalt silicates in the catalyst, but we would be hesitant to restrict the assignment to the Co_2SiO_4 formula. The DRIR spectrum of catalyst 13 (Fig. 5) showed weak carbonate peaks at 1500–1380 cm^{-1} and a shoulder around 1040 cm^{-1} that is assignable to cobalt silicates.

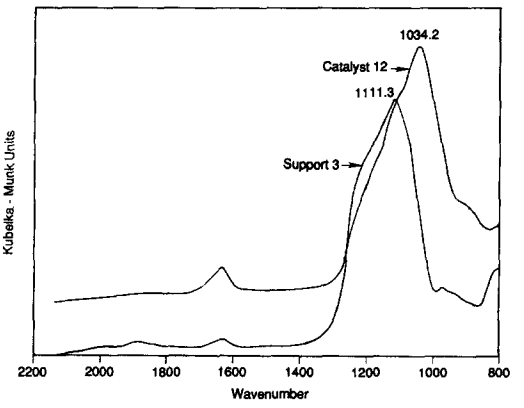

FIG. 4. Partial DRIR spectra of catalyst 12 and its support 3.

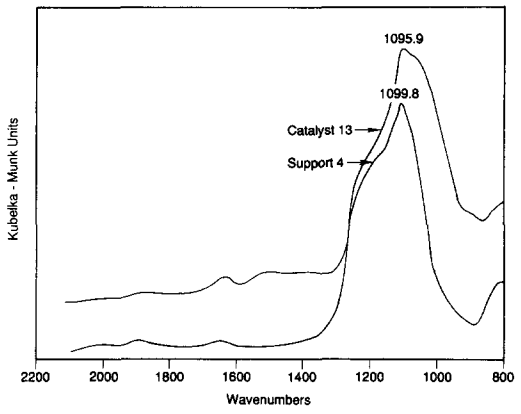

FIG. 5. Partial DRIR spectra of catalyst 13 and its support 4.

Clearly, in catalyst 13, part of the cobalt was present as carbonate and part of it as silicate.

The surface properties of the catalysts were also studied by XPS spectroscopy. The percentage cobalt reductions was determined by measuring the relative intensities of the elemental and the ionic Co $2p_{3/2}$ species at 777.7 and 781.0-eV binding energies after hydrogenations at 380°C, as shown in Table 3. Selected surface composition data acquired before and after hydrogenation of the catalyst are shown in Table 4. The surface and the bulk cobalt concentrations were similar. Some of the catalysts showed unexpectedly high surface carbon concentrations (see Table 4). Hydrogenations did not eliminate the surface carbon content. Since the sodium carbonate reagent can introduce carbonate species, the amounts of carbon species assignable to carbonate carbons (288.4 eV) are also shown in Table 4. Substantial amounts of carbonate carbons were found in catalysts 13 and 14, which were supported on diatomaceous earth. In catalyst 13, most of the carbonate carbon must have originated from the support, because the carbonate carbon content did not decrease upon reduction (see Table 4). In catalyst 14, the carbonate carbon content substantially decreased upon reduction, suggesting that a cobalt carbonate species was reduced with elimination of carbon dioxide.

Catalysts 12, 13, and 14 were examined by electron microscopy in combination with EDX analyses. Figures 6A and 6B show different areas of an electron micrograph of catalyst 12 and the EDX scans of the squared areas of the micrograph. The micrographs reveal a heterogeneous mixture consisting of clusters of various sizes, ranging from less than 0.1 to over 4 μm. Two types of cluster can be visually differentiated. The larger one appears very uniform in density and particle size, built up from tiny particles of less than 300 Å. This phase appears to be the "unaltered" silica support, as the EDX scans indicate by the nearly complete ab-

TABLE 4

Surface Cobalt and Surface Carbon Concentrations

Catalysts No.	Cobalt (wt%)		Surface composition (in atomic percent)					
	Surface	Bulk	As prepared			After H_2 treat (380°C)		
			Co	Total C	CO_3C	Co	Total C	CO_3C
10	12.4	18.0	3.9	26.6		1.1	14.8	
11	27.5	29.7	10.6	5.6	0.6	10.0	7.0	0.7
12	14.5	18.8	5.1	7.7	1.1	5.8	3.6	
13	25.5	17.6	9.6	15.3	8.7	8.5	22.0	13.4
14	37.8	17.7	14.3	22.5	7.9	15.1	25.5	2.6

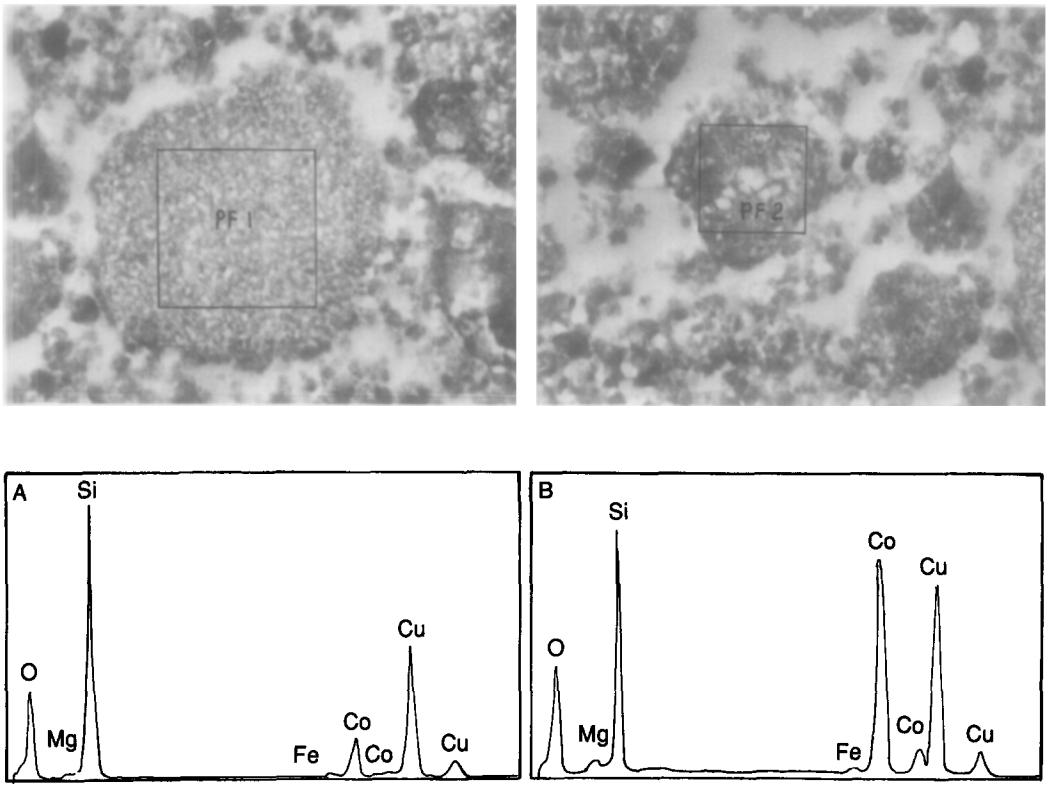

FIG. 6. Areas of electron micrographs and EDX scans of catalyst 12.

sence of Co (see Fig. 6A).The other type of clusters can be differentiated by higher density and a flocculent structure. The size of these clusters is usually smaller, up to about 1 μm. High levels of Co and Si were found in these by EDX (see Fig. 6B). At high magnifications, a filamentous structure with strand- and ribbon-like features is revealed. Large voids are present. The assumption of a cobalt silicate composition for this phase appears reasonable. In the EDX scans, a qualitative correlation seemed to exist between the Co and the Mg intensities. This suggests that the Co and the Mg stayed in proximity during and after the precipitation.

Figure 7 presents the electron micrograph of catalyst 13 at 155,000 magnification. Figure 8 shows the EDX scans of different areas or spots of the microtomed samples. In the micrograph, two distinctly different phases can be differentiated by visual inspection and by the aid of EDX scans. Large areas of the broken fragments of the diatomaceous earth support (up to several micrometers in size) remained "bare" and essentially intact. As illustrated in Fig. 8A, these areas showed little cobalt "contamination." Other areas of the support were covered with an irregular filamentous growth, with occasional regions of semiordered strands. EDX scans of these areas (see Figs. 8B and 8C) showed high concentrations of both Co and Si. It appears that the growth may be a reaction product of the silica (which in this particular case was the frustule of ancient diatoms) and of the cobalt reagent. Between the unreacted and reacted frustules, small clusters that did not appear to be associated with the much larger frustules were seen. Many of these small clusters were analyzed by EDX. All of them showed the presence

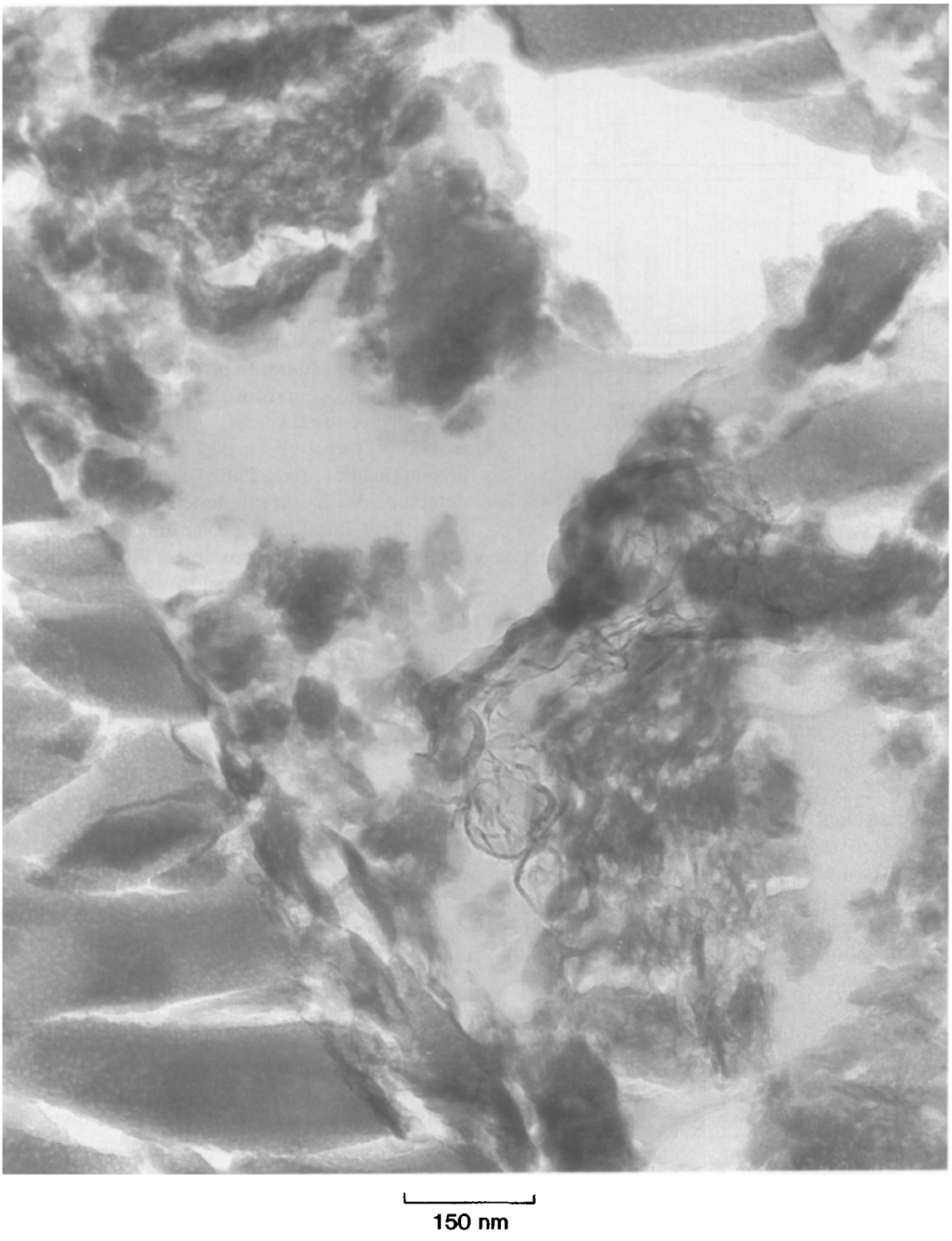

FIG. 7. Electron micrograph of catalyst 13 (×155,000).

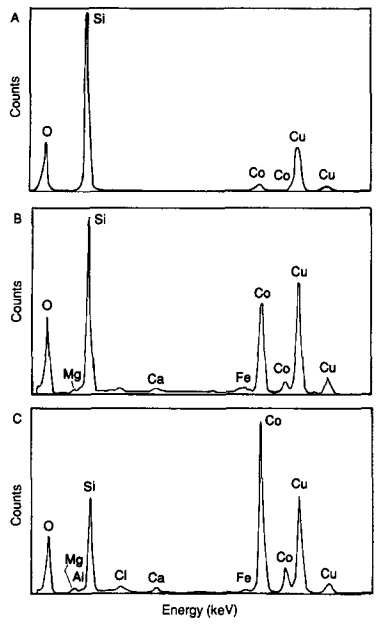

FIG. 8. EDX scans of different areas of a microtomed sample of catalyst 13.

of both Si and Co. Some were enriched in Co, but Si was also present. Clusters completely free of Si that could have been assigned to "unsupported catalyst" species were not found. We expected to find these species on the basis of IR and TPR analyses. Accordingly, the small clusters appear to be broken fragments from the "growths" on the frustules. The high Co content in some of these clusters may suggest that some of the broken growth fragments may have become admixed with the "unsupported catalyst" species during sample preparations.

The electron micrograph of catalyst 14 showed two distinctly different phases: the support and the catalyst. Little attachment was observed between the two phases.

DISCUSSION

When a solution of sodium carbonate is added to cobalt nitrate solution, a mixture of cobalt carbonates and cobalt hydroxide form (see Path 1 in Scheme 1). However, the reaction may follow an entirely different course if the precipitation occurs in the presence of magnesium nitrate and silica. In the extreme, using high-surface-area silica, all the cobalt can be converted to silicates. A combination of our analytical results (IR, TPR, EM–EDX, air-oxidation studies) has provided convincing evidence for the formation of cobalt silicates. However, the silicate-forming reaction is not well understood and the structures of the silicates formed are not known yet. The possible silicate structures are illustrated in Path 2 of Scheme 1. The surface area of the silica, which can be related to its reactivity, was found to be one determining factor on the course of the reaction. With high-surface-area silica, only Path 2-type reactions were observed. With low-surface-area silica, only Path 1 reactions were detected. With intermediate surface area silica, Path 1 and Path 2 reactions occurred simultaneously. The possible influence of other factors on the course of the reaction, including that of the Mg promoter, are currently under investigation.

The formation of cobalt silicates under the condition of our catalyst preparation was unknown and unexpected even though signs of such reaction (reducibility differences) were widely observed and reported. Of course, cobalt silicate formation from solutions of sodium silicate and cobalt salts is well known (*17*). Furthermore, the solid-state reaction of CoO with SiO_2 also gives cobalt silicates, but this reaction requires about 900°C temperature (*18*). In our system, the silica has a low solubility. There is a possibility that it may become solubilized during the course of the reaction. However, there must be a tremendous driving force for the silicate-forming reaction to compete with the alternative solute–solute reactions of Path 1. The silicas are known to be acidic, having ion-exchange properties (*19*). Some ionization may have occurred, and the siloxy anions, in the presence of Co^{2+} ions, may have initiated a chain reaction involving the depolymerization of the silica and reassembly into some form of cobalt silicate. The formation of

either monomeric or polymeric cobalt silicates may be possible (see Scheme 1). Literature reports on the stabilities of cobalt silicates (*20*) may lead to the expectations that the cobalt orthosilicate 19 may preferentially form. The possibility of surface cobalt silicate formation (23 to 25 in Scheme 1) was also considered but rejected on the basis of our EM–EDX studies that indicated an uneven Co–Si distribution. Finally, the possibility of Co–Mg–silicate formation should not be overlooked, even though the magnesium content of these catalysts was low (>5 Co : Mg atomic ratio).

For catalytic activity, the cobalt species present in the catalyst require reduction to zero-valent cobalt. Our TPR studies have indicated that the carbonate and the oxide species are readily reducible at relatively low temperatures, but the reduction of the silicate species requires high temperatures. In catalysts 10–12, 660–800°C was required for the reduction of the cobalt silicates, while in catalyst 13 the silicate reduction occurred in the 500–750°C range (compare Figs. 2c, 2d, and 2e). To explain the differences in the temperatures required for reduction of the silicates, one might assume that the silicate structures present in catalyst 13 are different than those in catalysts 10–12. For example, one might assume octahedral arrangement for the cobalt of catalyst 13 and tetrahedral sites in catalysts 10–12. This explanation would be in agreement with the published assignments of Roe *et al.* (*9*), who designated the reduction temperature regime around 520°C to the reduction of divalent, octahedral cobalt species. However, our experimental results support a different explanation. It was shown by a TPR study of blends that, in the presence of easily reducible cobalt species, the temperature required for the reduction of the cobalt silicate can be lowered, possibly due to hydrogen spillover. If this effect was demonstrable for macroscopic blends, it would be expected to be much more effective with "molecular blends," that is, with samples containing the two species in molecular proximity.

Finally, we express our hope that the contents of this paper provide a self-explanatory reason for the reproducibility difficulties reported for the preparation of the early commercial catalysts.

ACKNOWLEDGMENTS

Acknowledgments are due to P. R. Full, J. B. Hall, B. J. Huggins, J. A. Kaduk, R. S. Kurek, J. D. Northing, J. O. Schreiner, and C. M. Willey for their analytical contributions. F. L. Merenda of P. Q. Corporation is thanked for information on the surface properties of their silicas. C. W. Cain and J. Rimmer of Manville Corporation are thanked for their cooperation with the diatomaceous earth-supported catalysts. We also thank our referees for their stimulating comments.

REFERENCES

1. See, e.g., Minderhoud, J. K., and Post, M. F. M., US Patent 4,522,939 to Shell Oil Company, 1985.
2. For a review of the earlier literature, see Storch, H. H., Gulombic, N., and Anderson, R. B., "The Fischer–Tropsch and Related Syntheses." Wiley, New York, 1951; see p. 151 for the reproducibility of the catalyst preparations.
3. Anderson, R. B., Hall, W. K., Hewlett, H., and Seligman, B., *J. Am. Chem. Soc.* **69,** 3114 (1947).
4. Anderson, R. B., Hall, W. K., and Hofer, L. J. E., *J. Am. Chem. Soc.* **70,** 2465 (1948).
5. Reuel, R. C., and Bartholomew, C. H., *J. Catal.* **85,** 63 and 78 (1984).
6. Greegor, R. C., Lytie, F. W., Chin, R. L., and Hercules, D. M., *J. Phys. Chem.* **85,** 1232 (1981).
7. Viswanathan, B., and Gopalokrishnan, R., *J. Catal.* **99,** 342 (1986).
8. Sexton, B. A., Hughes, A. E., and Turney, T. W., *J. Catal.* **97,** 390 (1986).
9. Roe, G. M., Kidd, M. J., Cavell, K. J., and Larkins, F. P., *in* "Studies in Surface Science and Catalysis," Vol. 36, Methane Conversion, Proceedings of a Symposium on the Production of Fuels and Chemicals from Natural Gas, Auckland, April 27–30, 1987, p. 509. Elsevier, 1988.
10. Gruber, H. L., *Anal. Chem.* **13,** 1928 (1962).
11. Huffman, E. W. D., *Microchem. J.* **22,** 567 (1977).
12. Weller, S., *J. Am. Chem. Soc.* **70,** 799 (1948); also Weller, S., Hofer, L. J. E., and Anderson, R. B., *J. Am. Chem. Soc.* **70,** 799 (1948).
13. A. T. Bell, *Catal. Rev. Sci. Eng.* **23,** 203 (1981).
14. Wessner, D. A., Linden, G., and Bonzel, H. P., *Appl. Surf. Sci.* **26,** 355 (1986).
15. Gagnon, P. E., Cloutier, L., and Martineau, R., *Can. J. Res. B* **19,** 179 (1941).

16. Nyquist, R. A., and Kagel, R. O., "Infrared Spectra of Inorganic Compounds," No. 341. Academic Press, New York/London, 1971.
17. Schwarz, R., and Mathis, G. A., *Z. Anorg. Allg. Chem.* **126,** 55 (1923).
18. Ruger, M., *Ker. Rund.* **31,** 79, 87, 99, 110 (1923); *Chem. Abstr.* **18,** 156 (1924).
19. Burwell, R. R., Pearson, R. G., Heller, G. L., Tjok, P. B., and Chock, S. P., *Inorg. Chem.,* 1123 (1965).
20. Diev, N. P., and Gyribovskii, V. V., *J. Appl. Chem.* (USSR) **18,** 181, (1945); Morimoto, N., Tokonami, M., Watanabe, M., and Koto, K., *Am. Mineralogist* **23,** 475 (1974).